2021 IEEE 18th International Symposium on Biomedical Imaging (ISBI)
April 13-16, 2021, Nice, France

LOW-DOSE DUAL KVP SWITCHING USING A STATIC CODED APERTURE

Angela P. Cuadros[⋆]*, Carlos M. Restrepo*[⋆]*, and Peter Noël* [†]

[⋆] University of Delaware, Department of Electrical and Computer Engineering,
Newark, DE, USA, 19716
[†] Department of Radiology, Perelman School of Medicine,
University of Pennsylvania, Philadelphia, USA

2021 IEEE 18th International Symposium on Biomedical Imaging (ISBI) | 978-1-6654-1246-9/20/$31.00 ©2021 IEEE | DOI: 10.1109/ISBI48211.2021.9434080

ABSTRACT

This paper introduces a single-scan dual-energy coded aperture computed tomography system that enables material characterization at a reduced exposure level. Rapid kVp switching with a single-static block/unblock coded aperture relies on coded illumination with a plurality of X-ray spectra created by the kVp switching. Based on the tensor representation of the projection data, an algorithm to estimate the missing measurements in the tensor is proposed. This results in a full set of synthesized measurements that can be used with filtered backprojection or iterative reconstruction algorithms to accurately reconstruct the object in each energy channel. Simulation results validate the effectiveness of the proposed cost-effective solution to attain material characterization in low-dose dual-energy CT.

Index Terms— X-ray, Low-Dose, Tensor Completion.

1. INTRODUCTION

Computed tomography (CT) scanners reconstruct the linear attenuation coefficients of an object. These coefficients are a function of the material composition, the X-ray source effective energy, and the materials' mass density. Thus, materials with a different chemical composition can have the same linear attenuation coefficient in conventional CT reconstructions, which makes material characterization unfeasible [1]. To address these limitations, spectral CT uses measurements acquired at multiple energy spectra to quantify material composition. Currently, commercial dual-energy CT systems obtain two energy measurements by using sequential CT scans with different X-ray tube voltages, rapid kVp switching [2], a set of sandwiched detectors capable of discriminating between low and high X-ray energies [3], dual-source X-ray systems, or split-beam filtration. Then, material decomposition algorithms are used to identify particular materials or quantify their mass density. Furthermore, photon-counting detectors are recently being used in research settings to attain projection data at multiple energy channels to increase the spectral resolution. Yet, while these detectors are considered one of the future directions of CT technology, they are prohibitively expensive and are not yet applicable to practical cone-beam CT in large flat-panel forms [4].

The rapid increase in CT usage worldwide has led to concerns about future public health problems related to the CT radiation dosage. Thus, reducing radiation doses per CT scan has motivated major efforts from industry and academia to develop new approaches for attaining clinically useful images with the lowest possible radiation dose — methods referred to as low-dose CT [5]. Automatic tube-current reduction during gantry rotation and sparse-ray acquisition are two competing approaches. However, current implementations to attain sparse view sampling, such as switching the X-ray source on and off rapidly, are difficult to implement in practice [6]. The radiation doses in dual-energy systems are comparable to those attained in single-energy CT. However, reconstruction algorithms, as well as hardware that can aid in lowering the patient radiation dose, remain a topic of active research for both CT modalities. In our previous work [7], we explored a low-dose structured illumination system coined coded aperture compressive X-ray CT to address the aforementioned limitations in single energy CT. In this system, a static block/un-block 2D coded aperture is placed in front of the X-ray source to subsample the measurements at each angle position, effectively modifying the sensing matrix. The implementation of these strategies in multi-energy systems, however, is especially challenging since the accuracy of the material decomposition stage decreases when low-dose systems are used to obtain the X-ray data. Comparison of the proposed approach and state of the art inpainting methods can be found in [7]. In this paper, we apply the structured illumination concept to low-dose dual energy systems and develop a reconstruction framework to solve the resulting ill-posed inverse problem. Namely, we propose the use of a single static coded aperture together with a rapid kVp switching system. Given the set of spectrally multiplexed measurements, we propose an alternative reconstruction framework in which we exploit the correlation of the data in the projection space to estimate the measurements in the incomplete projection data tensor constructed by stacking the sinogram measurements obtained at each energy. This results in synthesizing a full

set of measurements that can be used by conventional reconstruction algorithms. Then, using the plurality of spectra, material differentiation can be attained without sacrificing image quality.

2. FORWARD MODEL

For simplicity, a fan-beam X-ray CT system is considered. However, the generalization to cone-beam CT and other 3D geometries is straightforward. The X-ray source travels in a circular trajectory around the object, and X-ray projections are measured at different angles using a line detector with Q detector elements. At each detector position j, the measurements are given by Beer-Lambert's law of attenuation $I_j = \int_E I_{0j}(E) \exp\left(-\int_\ell \mu(\ell, E) d\ell\right) dE$, where $I_{0j}(E)$ is the impinging X-ray photon intensity at energy E, $\mu(\ell, E)$ is the linear attenuation coefficient of the object at position ℓ and energy E, and $j = 1, \cdots, QP$ where P is the number of angles at which projections are taken. For simplification, in single energy CT, the measured intensity is written in terms of the effective energy $\bar{E}$, i.e., the energy of a monoenergetic source that would produce the same measurements as the poly-energetic source. Mathematically, the post-log data is then given by $\mathbf{y}_j = \ln\left(I_{0j}(\bar{E})/I_j\right) = \int_\ell \mu(\ell, (\bar{E})) d\ell$. In real systems, only a discrete number of measurements are available, thus the imaging model needs to be discretized. For an object of dimensions $N \times N$, the line integral projections are attenuated by the object as described by the ray path $\mathbf{H}_j$, that is, $\mathbf{y}_j = \mathbf{H}_j \mathbf{x}$, where $\mathbf{x} \in \mathbb{R}^{N^2}$ is a vectorized representation of the linear attenuation coefficients of the object. Thus, the discrete-to-discrete formulation can be written as a finite linear system of equations of the form $\mathbf{y} = \mathbf{H}\mathbf{x}$, where $\mathbf{H} \in \mathbb{R}^{QP \times N^2}$ is the system matrix, with $\mathbf{H}_{ij}$ equal to the intersection length of the j^{th} ray with the i^{th} voxel for $i = 1, \cdots, N^2$, and $\mathbf{y} \in \mathbb{R}^{QP \times 1}$ is a vector containing all the measurements. Multiple algorithms such as filtered back-projection (FBP) can then be used to obtain the effective linear attenuation coefficients of the object.

In single energy CT, however, materials having different compositions may be represented by the same gray-scale value. Hence, material differentiation can be very challenging. Spectral CT relies on the energy and material dependence of X-ray linear attenuation coefficients. Namely, measurements obtained with different effective energies can be used to differentiate between multiple materials. In dual-energy systems, two sets of data, one corresponding to a high energy spectrum and a second one using a low-energy spectrum, are acquired. Mathematically, let the reconstructed linear attenuation coefficients at pixel i be denoted as x_i^L and x_i^H, for the low and high energies respectively. Then the material decomposition can be formulated as follows:

$$\begin{pmatrix} x_i^H \\ x_i^L \end{pmatrix} = \begin{pmatrix} \mu^{1H} & \mu^{2H} \\ \mu^{1L} & \mu^{2L} \end{pmatrix} \begin{pmatrix} \rho_i^1 \\ \rho_i^2 \end{pmatrix}, \quad (1)$$

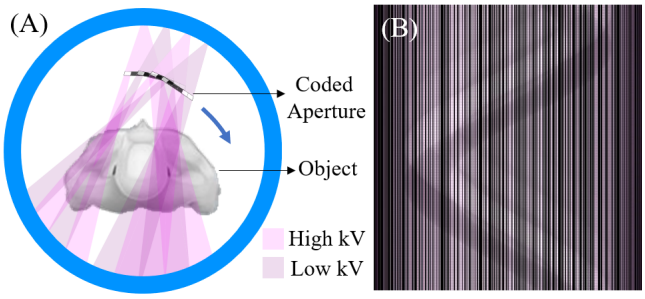

Fig. 1. Rapid kVp switching using a single coded aperture: (A) system schematic and (B) interleaved sinogram.

where ρ_i^m represents the concentration of the m^{th} basis material in the object at the i^{th} pixel and $\mu^{mH/L}$ is defined as the effective mass attenuation coefficient of each base material $m = 1, 2$ measured at the corresponding energy spectrum. The latter is obtained as follows $\mu^{mc} = \sum_k^K S^c(E_k)\mu_m(E_k) / \sum_k^K S^c(E_k)$, where $S^c(E_k)$ is the system spectral response to the energy channel c at energy E_k for $k = 1, \ldots, K$, and K is the number of energy bins. Then, using the basis materials and the reconstructed pixel values at both high and low kVp, the material decomposition can be performed using the straightforward matrix inversion of (1) for each pixel independently.

2.1. Rapid kVp Switching Using a Single Coded Aperture

Figure 1(A) depicts the rapid kVp switching coded aperture system for a fan beam geometry. Similar to the work presented in [7], a static block/unblock coded aperture is placed in front of the X-ray source. However, in this case, the tube potential alternates between consecutive views between high and low energy to attain the dual-energy-data. The acquired projection dataset is thus an interleaved coded sinogram, and since the coded aperture is static, entire columns of the sinogram, corresponding to the blocking coded aperture elements, are not observed as depicted in Fig. 1(B). Mathematically, the inverse problem can be formulated independently for each X-ray tube potential as follows:

$$\hat{\mathbf{x}}^c = \underset{\mathbf{x}^c}{\operatorname{argmin}} \|\mathbf{y}^c - \mathbf{C}^c \mathbf{H} \mathbf{x}^c\|_2^2 + \lambda \|\mathbf{x}^c\|_p, \; c = \{\mathrm{L}, \mathrm{H}\} \quad (2)$$

where $\hat{\mathbf{x}}^c$ are the effective linear attenuation coefficients in the energy channel c (L = Low, H = High), λ is a regularization constant, $\|\cdot\|_2$ corresponds to the ℓ_2 norm, and $\|\cdot\|_p$ represents any prior information about the data. The binary matrix, $\mathbf{C}^c = [\mathbf{c}_1^c, \mathbf{c}_2^c, \cdots, \mathbf{c}_{QP}^c]$ accounts for the kVp switching as well as for the coded aperture. To that end, the column vector $\mathbf{c}_j^c \in \mathbb{R}^{D_c \times 1}$ is a zero vector if the j^{th} detector element is associated with a blocking coded aperture element or the angle associated with j does not correspond to the energy channel c; otherwise $\mathbf{c}_j^c$ belongs to the natural basis in $\mathbb{R}^{D_c \times 1}$,

where D_c is the number of unblocked elements in the c^{th} energy channel. Since the measurements are not multiplexed in the detector array, the vectors $\mathbf{c}_j^c$ are disjoint. The theory of compressed sensing (CS) indicates that the best results make use of completely random measurements [8]. However, since a single coded aperture is used in all the view angles the sampling density distribution of the proposed system presents multiple rings of high and low sensing density, and some pixels in the center of the image are not sensed [7], which produces artifacts in the reconstructions. Thus, rather than using iterative CS reconstruction algorithms directly on the observed measurements to solve (2), the approach taken in this work is to formulate the sensing problem in a tensorial form and estimate the missing projection data based on the tensor representation of the measurements. Namely, the missing entries in the 3D tensor representation of the projection data are estimated using a tensor completion algorithm. Then conventional algorithms can be used for fast image reconstruction in each channel, given that a complete set of measurements is available. Finally, using (1) on a pixel-by-pixel basis, image domain material decomposition can be performed or since the complete projection data is available, projection data approaches can be applied as well.

3. IMAGE RECONSTRUCTION USING TENSOR COMPLETION

Based on the low-rank tensor completion minimization developed in [7], a 3D tensor representation of the spectral projection data can be obtained for the proposed system. For a fan-beam CT system using a $Q \times 1$ line detector and a full circle scan with P view angles, the measurements' tensor is defined as $\mathcal{Y} \in \mathbb{R}^{P \times Q \times C}$, where C is the number of available energy channels. Figure 2 depicts the 3D tensor for a rapid kVp switching dual-energy system using a single coded aperture, obtained by stacking the $C = 2$ tiled subsampled sinograms corresponding to the low and high energies which correspond to the frontal slices of the tensor. Note, when using a single-static coded aperture the rows of the sinograms will exhibit the same blocking pattern, which results in vertical lines of missing data in the frontal slices of the tensor at the locations corresponding to the coded aperture blocking elements. Furthermore, the kVp switching between angles results in interleaved missing rows between the measured projections. The fan-beam sinograms that make the frontal slices are gray-scale images that can be considered low-rank when a large number of angles are used. Furthermore, when a coded aperture is placed in front of the X-ray source, the sinograms can be seen as a set of images with missing patches. Thus, the missing measurements can be estimated using image inpainting techniques such as matrix completion for each energy channel:

$$\hat{\mathbf{Y}}^{\,c} = \underset{\mathbf{Y}^c}{\operatorname{argmin}} ||\mathbf{Y}^c||_* \text{ s.t. } \mathbf{Y}^c_{ij} = \mathbf{O}^c_{ij}\ (i,j) \in \Omega, \qquad (3)$$

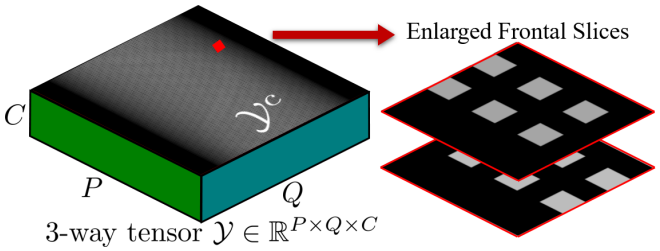

Fig. 2. Tensor representation of phantom projection data obtained using a static coded aperture and kVp switching.

where $\hat{\mathbf{Y}}^{\,c}$ is the estimated sinogram at energy channel c, $||\cdot||_*$ is the nuclear norm, $\mathbf{O}^c$ are the partially observed measurements, and Ω is the set of indices of the observed entries. This matrix formulation, however, ignores the multidimensional structure of the measurements. Furthermore, the sinograms obtained in both systems have entire columns of missing data making the measurement estimation extremely challenging using matrix completion [9]. Considering the tensor across all dimensions, on the other hand, provides a more natural and compact representation of the data and allows the usage of the tensor completion framework to estimate the unobserved measurements. Thus, the measurement estimation is formulated as a low-rank tensor completion problem:

$$\hat{\mathcal{S}} = \underset{\mathcal{S}}{\operatorname{argmin}} ||\mathcal{S}||_{\text{TNN}} + \lambda \Phi(\mathcal{S}) \text{ s.t. } \mathcal{P}_\Omega(\mathcal{S}) = \mathcal{P}_\Omega(\mathcal{Y}), \quad (4)$$

where $\hat{\mathcal{S}}$ is the estimate of the projection data tensor, $\mathcal{Y}$ is the observed incomplete tensor, $\mathcal{P}_\Omega(\mathcal{Y}) = \mathcal{Y}(i,j,k)$ for $(i,j,k) \in \Omega$, otherwise $\mathcal{P}_\Omega(\mathcal{Y}) = 0$, $||\cdot||_{\text{TNN}}$ is the tensor nuclear norm, and Ω is the set of indices of the observed entries. The data-driven regularization term $\Phi(\mathcal{S})$ is added to capture fine details in the reconstructed tensor that may not be well-captured by the low-rank regularizer. In this work, the ADMM framework developed in [10] is used to solve (4) and obtain an estimation of the measurements' tensor. At this point, any analytical reconstruction algorithm may be used to reconstruct the object given that a complete set of fan-beam CT measurements is available. In this work, the FBP algorithm is used to reconstruct the effective linear attenuation coefficients at each energy c using the corresponding estimated sinogram $\hat{\mathcal{S}}^c$, that is the c^{th} frontal slice of the estimated measurement tensor.

4. SIMULATION STUDY

Figure 3 depicts the X-ray spectra simulated using Spektr [11], for the low and high kVp tube potentials of a rapid kVp switching system with inherent filtration of 1.6 mm of aluminum. The peaks were set to 80 and 140 kV and were modified by filtration with 2.0 mm of aluminum and 0.2 mm of copper. The proposed approach is tested to determine its capability of decomposing water and iodine using a 256×256

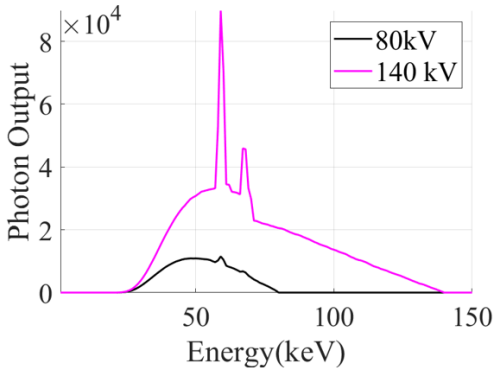

Fig. 3. kVp switching spectra

iodine sensitivity phantom of 20 cm side length, composed of a water cylinder and a set of 8 vials with varying iodine concentration, see Table 1 and Figs. 4 (A-B). The ASTRA tomography toolbox [12] is used to simulate a fan beam X-ray CT configuration with a flat 1D, 40 cm detector strip composed of $Q = 1024$ elements, and distances from the source to the center of rotation and the detector of 40 cm and 80 cm respectively. The hardware settings of the experiment are calculated based on [13]. The mass attenuation coefficients for iodine and water, were obtained from the National Institute of Standards and Technology (NIST) X-ray attenuation databases [14]. Peak kV was switched every projection. The same coded aperture was used in $P = 1372$ view angles uniformly spread over 360 degrees. The coded aperture had a Bayer structure with 37.5% transmittance, that is, 384 of its elements let the X-rays pass. For comparison, a sparse view angle system with rapid kVp switching and $P = 514$ view angles for equivalent radiation dosage was simulated as well. Figures 4 (C-D) depict the material decomposition results for the proposed approach, and Figs. 4(E-F) depict the material decomposition results for the sparse view angle system with rapid kVp switching. Note, the latter reconstructions contain more noise than the proposed system's reconstructions. Furthermore, low concentrations of iodine are closer to the original value in the proposed method as shown in Table 1. In both systems, FBP is used to reconstruct the effective energy linear attenuation coefficients in each energy channel, then a constrained least-squares algorithm is used to solve the material decomposition problem for each pixel independently.

Table 1. Average concentration in the phantom vials.

Fig.	Iodine concentration (mg/ml)							
4 (B)	4	3	2	1	0.75	0.5	0.25	0.1
4 (D)	3.5	2.6	1.7	0.7	0.5	0.3	0.2	0.2
4 (F)	3.6	2.8	1.9	1.2	0.9	0.8	0.7	0.7

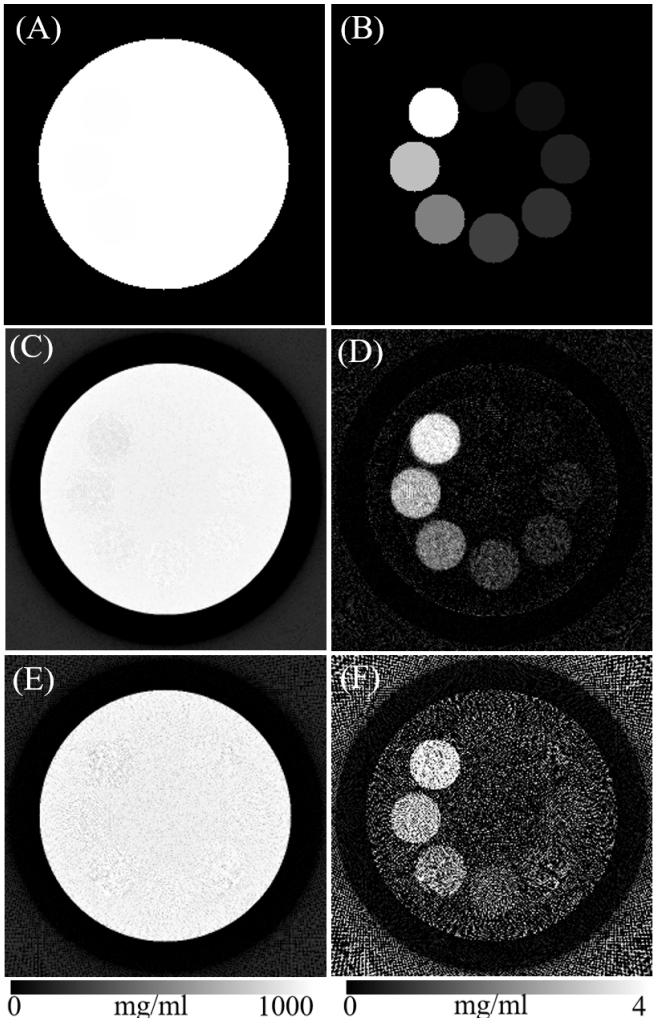

Fig. 4. Water-iodine material decomposition: (A-B) Reference. FBP reconstructions for rapid kVp switching and (C-D) 37.5% transmittance coded apertures, (E-F) sparse angles.

5. CONCLUSIONS AND FUTURE WORK

The proposed coded aperture architecture represents a radical departure from conventional methods used in dual-energy X-ray CT to reduce the radiation dose levels. The structured X-ray illumination is projected through the objects of interest and measured with standard X-ray energy integrating detectors. Then, we used tensor completion algorithms to estimate the missing measurements in each energy channel, which results in a synthesized full set of measurements that can be used with conventional CT reconstruction algorithms. Thus, providing a cost-effective solution for low-dose dual-energy systems. The methods developed in this paper can be directly applied to obtain material decomposition using other dual energy architectures and system geometries by adapting the proposed measurement's tensor. The latter is a topic of current research.

6. COMPLIANCE WITH ETHICAL STANDARDS

This is a numerical simulation study for which no ethical approval was required.

7. ACKNOWLEDGMENTS

This work was supported in part by the National Science Foundation under Grant CIF 1717578, by the University of Delaware under a Blue Hen Proof of Concept Grant, and a UNIDEL grant.

8. REFERENCES

[1] Cynthia H. McCollough, Shuai Leng, Lifeng Yu, and Joel G. Fletcher, "Dual- and multi-energy ct: Principles, technical approaches, and clinical applications," *Radiology*, vol. 276, no. 3, pp. 637–653, Sept. 2015.

[2] Xiaoye Wu, David A. Langan, Dan Xu, Thomas M. Benson, Jed D. Pack, Andrea M. Schmitz, Eric J. Tkaczyk, Jaynne Leverentz, and Paul Licato, "Monochromatic CT image representation via fast switching dual kVp," in *Medical Imaging 2009: Physics of Medical Imaging*, Ehsan Samei and Jiang Hsieh, Eds. International Society for Optics and Photonics, 2009, vol. 7258, pp. 1302 – 1310, SPIE.

[3] Derek S Tsang, Thomas E Merchant, Sophie E Merchant, Hanna Smith, Yoad Yagil, and Chia-Ho Hua, "Quantifying potential reduction in contrast dose with monoenergetic images synthesized from dual-layer detector spectral ct," *The British Journal of Radiology*, vol. 90, no. 1078, pp. 20170290, 2017.

[4] D. Lee, J. Lee, H. Kim, T. Lee, J. Soh, M. Park, C. Kim, Y. J. Lee, and S. Cho, "A feasibility study of low-dose single-scan dual-energy cone-beam ct in many-view under-sampling framework," *IEEE Transactions on Medical Imaging*, vol. 36, no. 12, pp. 2578–2587, 2017.

[5] J. Z. Liang, P. J. La Riviere, G. El Fakhri, S. J. Glick, and J. Siewerdsen, "Guest editorial low-dose ct: What has been done, and what challenges remain?," *IEEE Transactions on Medical Imaging*, vol. 36, no. 12, pp. 2409–2416, Dec 2017.

[6] Matthew J Muckley, Baiyu Chen, Thomas Vahle, Thomas O'Donnell, Florian Knoll, Aaron D Sodickson, Daniel K Sodickson, and Ricardo Otazo, "Image reconstruction for interrupted-beam x-ray CT on diagnostic clinical scanners," *Physics in Medicine & Biology*, vol. 64, no. 15, pp. 155007, aug 2019.

[7] A. P. Cuadros, X. Liu, P. Parsons, X. Ma, and G. R. Arce, "Single-static coded aperture x-ray ct: Image reconstruction and experimental demonstration," *IEEE Transactions on Computational Imaging*, submitted for publication.

[8] David J. Brady, Alex Mrozack, Ken MacCabe, and Patrick Llull, "Compressive tomography," *Adv. Opt. Photon.*, vol. 7, no. 4, pp. 756–813, Dec 2015.

[9] E. J. Candes and B. Recht, "Exact low-rank matrix completion via convex optimization," in *2008 46th Annual Allerton Conference on Communication, Control, and Computing*, Sep. 2008, pp. 806–812.

[10] Xi-Le Zhao, Wen-Hao Xu, Tai-Xiang Jiang, Yao Wang, and Michael K. Ng, "Deep plug-and-play prior for low-rank tensor completion," *Neurocomputing*, 2020.

[11] J. H. Siewerdsen, A. M. Waese, D. J. Moseley, S. Richard, and D. A. Jaffray, "Spektr: A computational tool for X-ray spectral analysis and imaging system optimization," *Medical Physics*, vol. 31, no. 11, pp. 3057–3067, 2004.

[12] Wim van Aarle, Willem Jan Palenstijn, Jeroen Cant, Eline Janssens, Folkert Bleichrodt, Andrei Dabravolski, Jan De Beenhouwer, K. Joost Batenburg, and Jan Sijbers, "Fast and flexible x-ray tomography using the astra toolbox," *Opt. Express*, vol. 24, no. 22, pp. 25129–25147, Oct 2016.

[13] Yan Kaganovsky, Daheng Li, Andrew Holmgren, HyungJu Jeon, Kenneth P. MacCabe, David G. Politte, Joseph A. O'Sullivan, Lawrence Carin, , and David J. Brady, "Compressed sampling strategies for tomography," *J. Opt. Soc. Am. A 31*, 2014.

[14] J.H. Hubbell and S.M. Seltzer, "Radiation and biomolecular physics division, MPL NIST," `https://physics.nist.gov/PhysRefData/XrayMassCoef/tab3.html`, Accessed March 1, 2018.